Supporting information

Silica Restricting the Sulfur Volatilization of Nickel Sulfide for High-Performance Lithium-Ion Batteries

Qidong Li, Li Li, Peijie Wu, Nuo Xu, Liang Wang, Matthew Li, Alvin Dai, Liqiang Mai, Jun Lu,* and Khalil Amine*

Q. D. Li, L. Li, P. J. Wu, N. Xu, Prof. L. Q. Mai
State Key Laboratory of Advanced Technology for Materials Synthesis and

Processing International School of Materials Science and Engineering, Wuhan

University of Technology
Wuhan, 430070, Hubei, China. E-mail: mlq518@whut.edu.cn

Q. D. Li, M. Li, A. Dai, Dr. J. L., Dr. K. A.
Chemical Sciences and Engineering Division, Argonne National Laboratory, 9700 South Cass Avenue, Lemont, IL, 60439, USA. E-mail: junlu@anl.gov

L. Wang
Department of Physics, Northern Illinois University, Dekalb, IL, 60115, USA

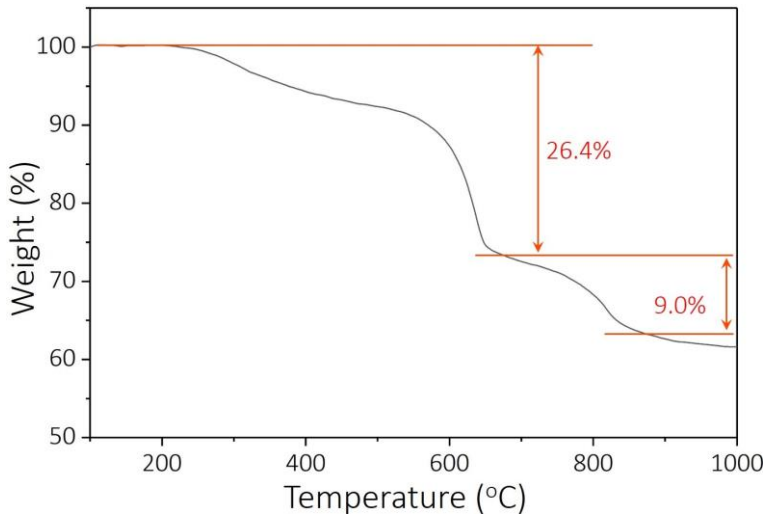

Figure S1. TGA curves of NiS_2.

Table S1. Elementary analysis with Inductive Coupled Plasma Emission Spectrometer (ICP) for Ni and S contents in the NiS_x@C sample.

	Concentration	Unit	wt%	Mole ratio (S/Ni)
Ni 231.604 r	210.9626	mg L^{-1}	43.9645	1.23
S 180.731 r	142.4983	mg L^{-1}	29.6966	

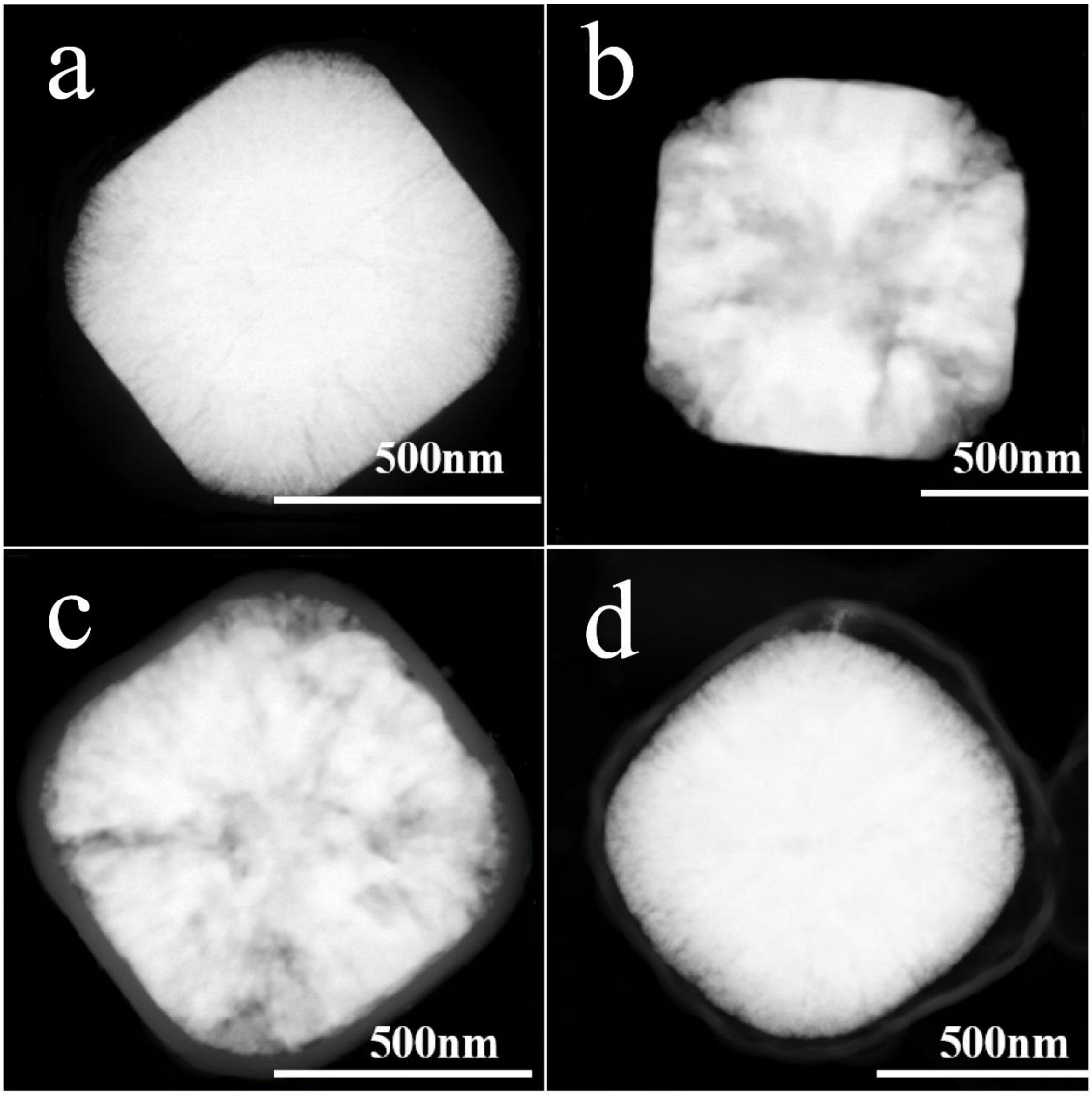

Figure S2. HAADF images of (a) NiS_2, (b) NiS-600, (c) NiS/C-600 and (d) NiS_x@C yolk-shell microboxes.

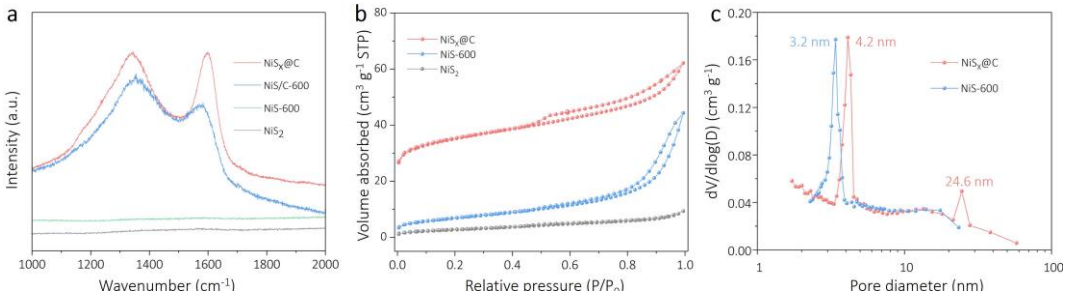

Figure S3. a) Raman spectra of NiS_2, NiS-600, NiS/C-600 and NiS_x@C. b) N_2 adsorption/desorption isotherm of NiS_2, NiS-600 and NiS_x@C. c) Pore size distribution curves NiS-600 and NiS_x@C.

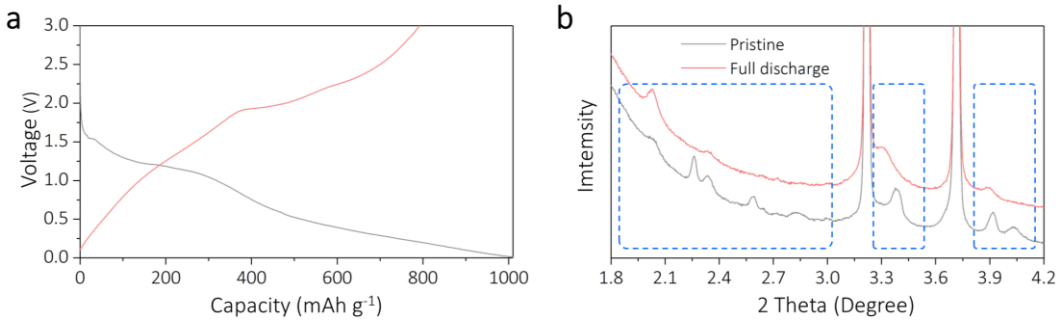

Figure S4. a) Initial discharge/charge curve of NiS_x@C electrode. b) *In-situ* synchrotron HEXRD of NiS_x@C electrode at pristine and full discharge state.

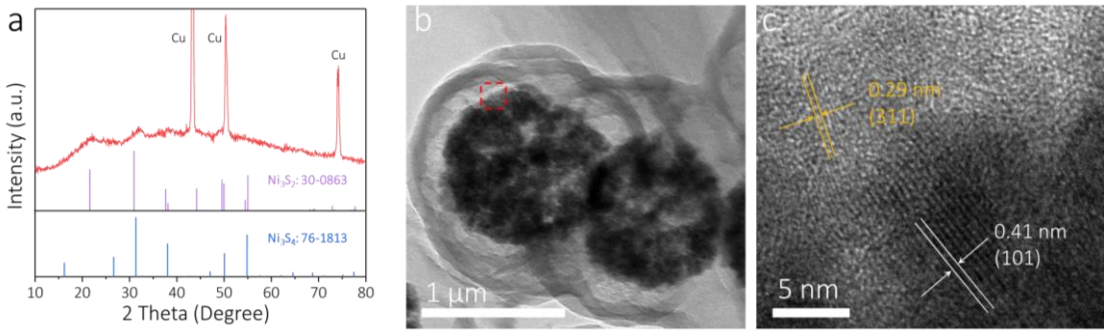

Figure S5. a) XRD pattern, b) TEM image, and c) HRTEM image of NiS_x@C electrode after first charge process.

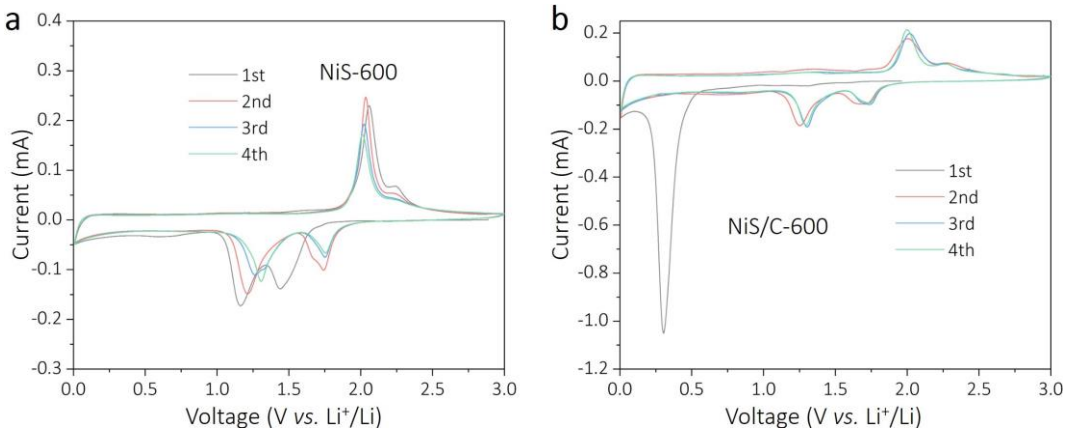

Figure S6. a) Cyclic voltammograms of NiS-600 and b) NiS/C-600 at a scan rate of 0.1 mV s^{-1}.

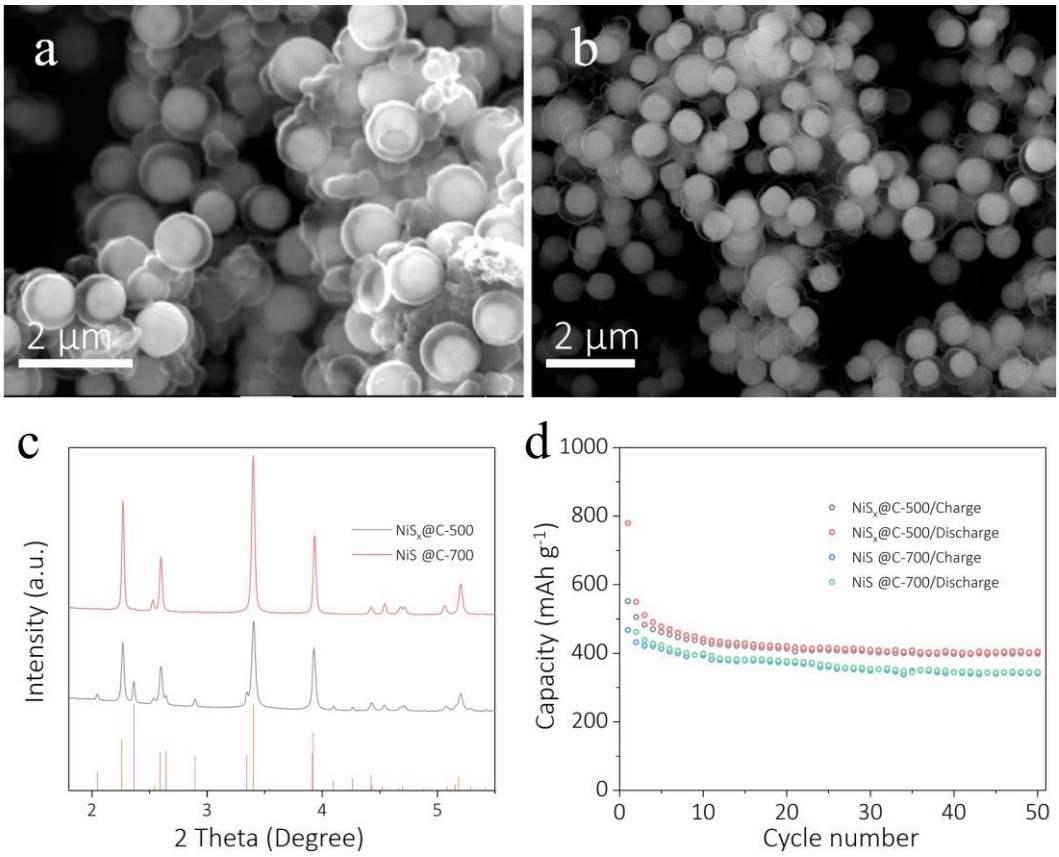

Figure S7. SEM images of NiS_x@C-500 (a) and NiS@C-700 (b). c) HEXRD of NiS_x@C-500 and NiS@C-700. d) Cycling performance of NiS_x@C-500 and NiS@C-700 at 1 A g^{-1}.

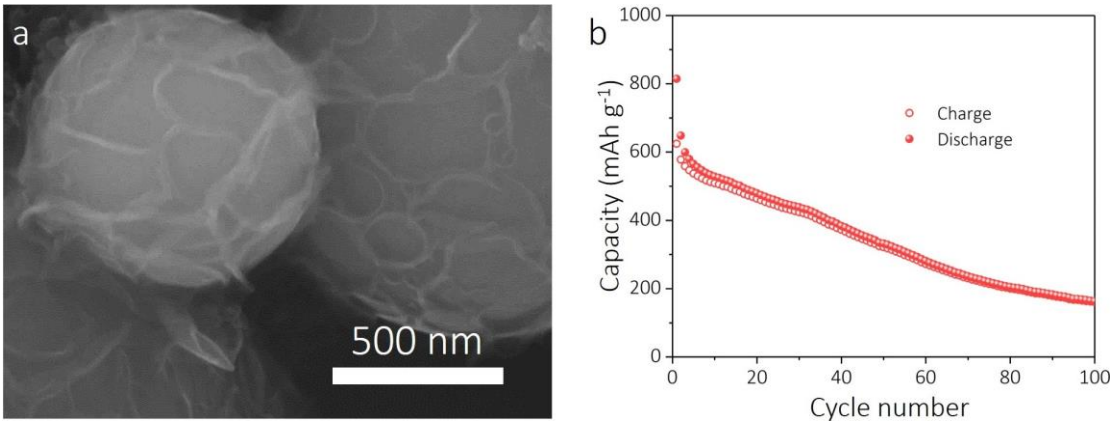

Figure S8. a) SEM images of NiS_x@C-T. b) Cycling performance of NiS_x@C-T at 1 A g^{-1}.

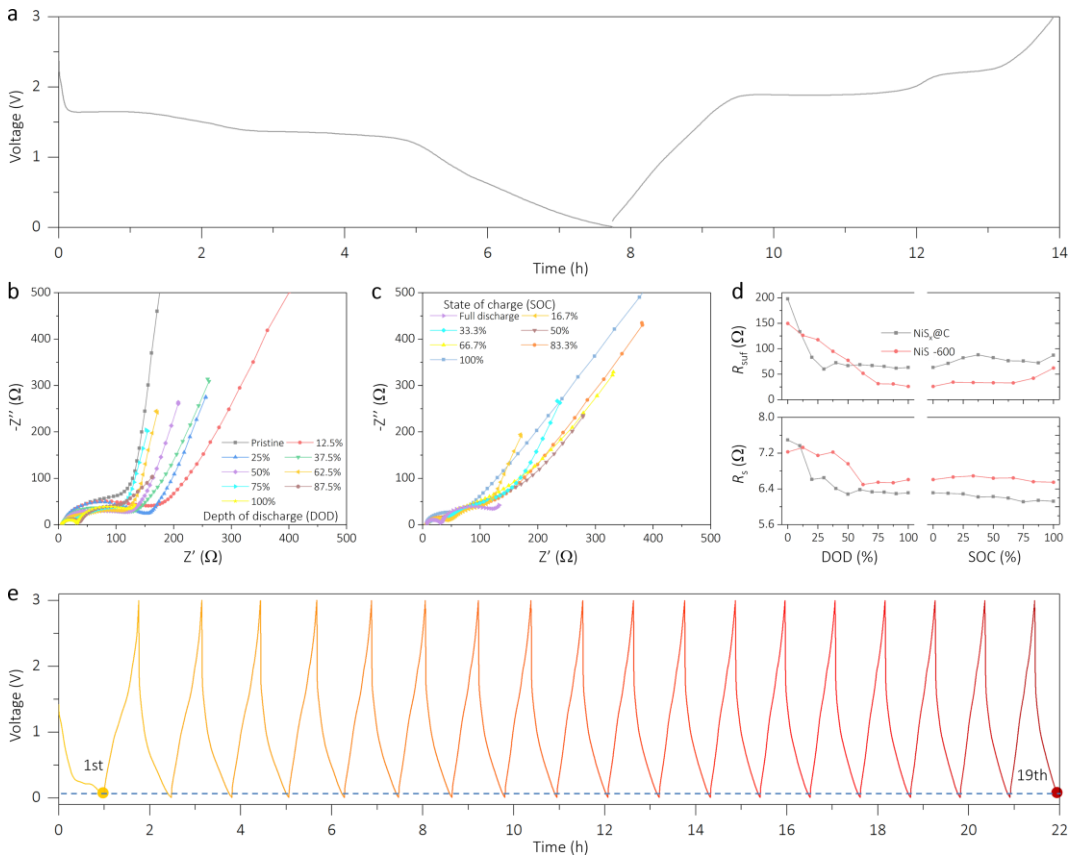

Figure S9. a) Initial discharge/charge curve of NiS-600 electrode for *in-situ* EIS tests. *In-situ* time-lapse EIS profiles of NiS-600 electrode at different depths of discharge (DOD) (b) and different states of charge (SOC) (c) during the initial discharge/charge. d) Plots of electrolyte solution resistance (R_s) and R_{suf} against SOC and DOD. e) Discharge/charge curve of NiS_x@C electrode for *in-situ* EIS tests at 1 A g^{-1}.

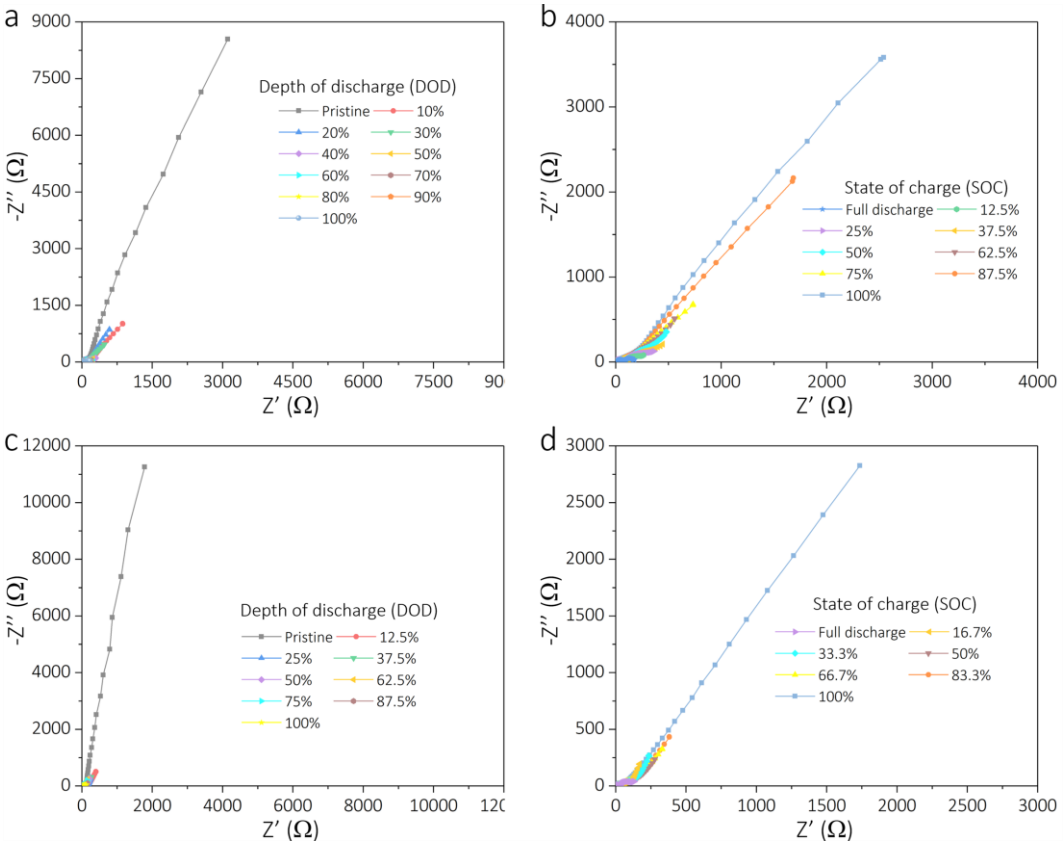

Figure S10. (a-b) Full *in-situ* EIS profiles of NiS_x@C electrode at first discharge/charge process. (c-d) Full *in-situ* EIS profiles of NiS-600 electrode at first discharge/charge process.

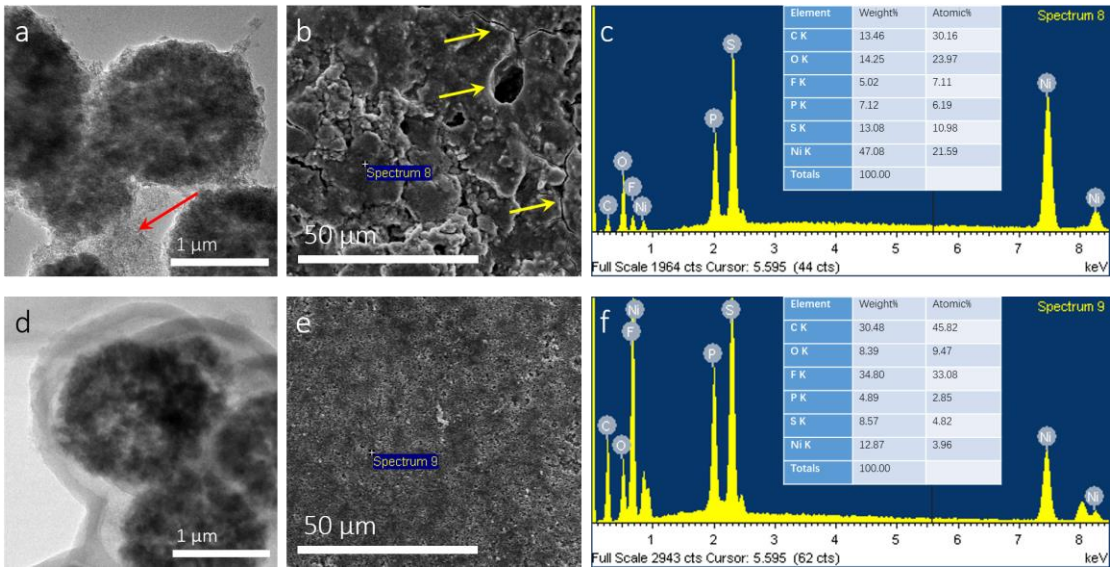

Figure S11. (a-c) TEM and EDS analysis of NiS-600 electrode after 30 cycles at full charge state. (d-f) TEM and EDS analysis of NiS_x@C electrode after 30 cycles at full charge state.

a

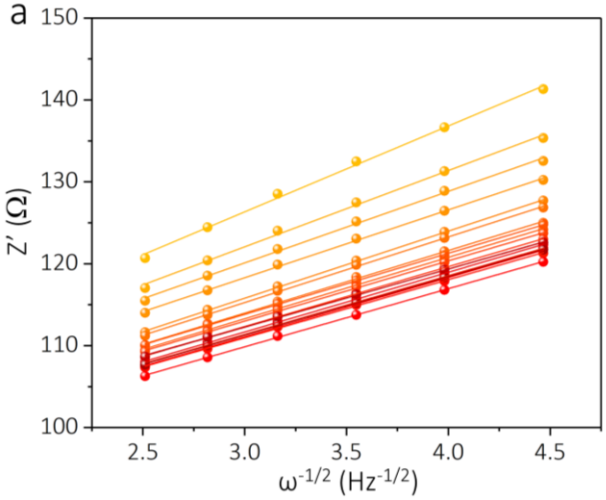

b

Cycle No.	Slope	Cycle No.	Slope
1	10.4848	11	7.31616
2	9.31251	12	7.27439
3	8.73779	13	7.19931
4	8.28994	14	7.1321
5	8.1929	15	7.09826
6	8.01214	16	7.09007
7	7.6382	17	7.06275
8	7.50139	18	7.1023
9	7.44946	19	7.09461
10	7.35818		

Figure S12. (a) Relationship between Z_{re} and $\omega^{-1/2}$ in the low frequency region for the NiS_x@C electrode. (b) Fitting slope of different cycles.

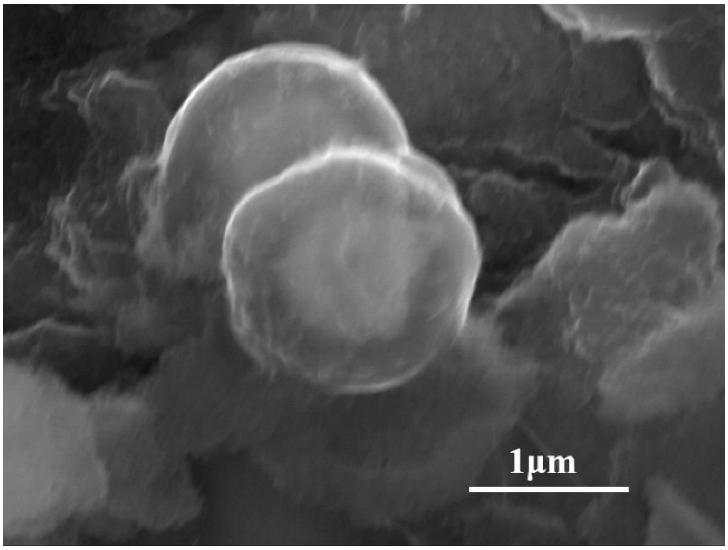

Figure S13. SEM image of NiS_x@C yolk-shell microboxes electrode after 2000 cycles at 1 A g^{-1}.

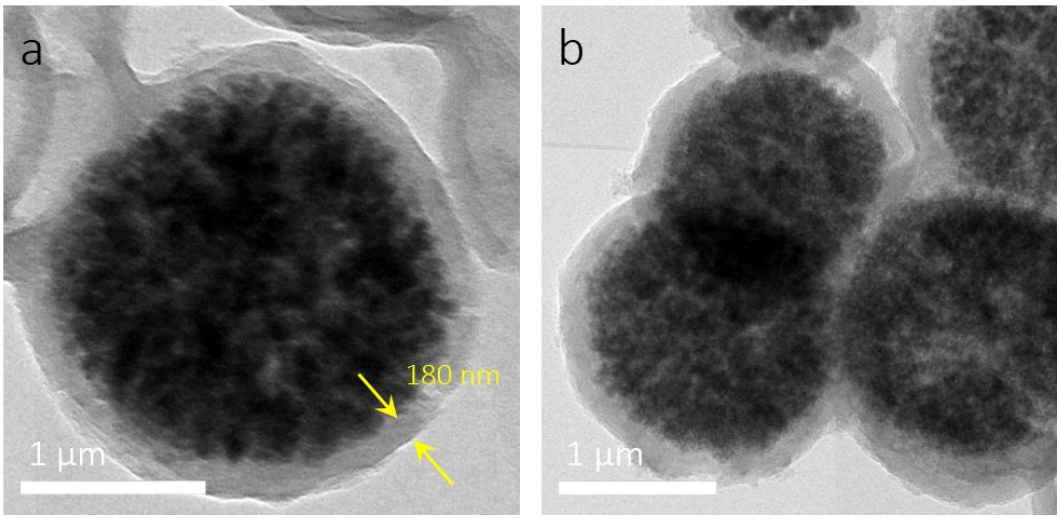

Figure S14. a) TEM image of NiS_x@C electrode after 3 cycles at full discharge state. b) TEM image of NiS_x@C electrode after 30 cycles at full discharge state.

Table S2. Elementary analysis of N, C, H, and S contents in the NiS_x@C and NiS/C-600.

Sample	N(%)	C(%)	H(%)	S(%)
NiS_x@C	0.59	29.91	0.133	30.488
NiS/C-600	0.6	29.31	0.031	25.745